ELSEVIER

Applied Surface Science 186 (2002) 14–23

applied surface science

www.elsevier.com/locate/apsusc

Novel applications for laser ablation of photopolymers

T. Lippert[a,*], C. David[a], M. Hauer[a], T. Masubuchi[b], H. Masuhara[b], K. Nomura[b], O. Nuyken[c], C. Phipps[d], J. Robert[c], T. Tada[b], K. Tomita[b], A. Wokaun[a]

[a]*Paul Scherrer Institut, 5232 Villigen PSI, Switzerland*
[b]*Osaka University, Suita, Osaka 565-0871, Japan*
[c]*Technische Universität München, Lichtenbergstr. 4, 84747 Garching, Germany*
[d]*Photonic Associates, 200A Ojo de la Vaca Road, Santa Fe, NM 87504, USA*

Abstract

The ablation characteristics of various polymers were studied at low and high fluences. The polymers can be divided into three groups, polymers containing triazene groups, polyesters with cinnamylidenemalonyl groups, and polyimide (PI) as reference polymer. The polymers containing the photochemically most active group (triazene) are also the polymers with the lowest threshold of ablation and the highest etch rates, followed by the designed polyesters and then PI. The triazene-polymer (TP) was studied at low fluences with additional techniques. UV–Vis spectroscopy and TOF-MS reveal that the triazene-chromophore decomposes also upon irradiation with fluences below the threshold of ablation. At the threshold fluence, a pronounced change is detected, i.e., an approximately 10 times higher decomposition rate. Nanosecond surface interferometry was applied to detect changes of the surface morphology of the TP and PI after irradiation with fluences above the threshold of ablation. In the case of the TP, no swelling of the surface is observed and etching starts and ends with the laser pulse, while a very pronounced swelling is detected for PI. The clear difference between PI and the designed polymers can be explained by a pronounced thermal part in the ablation mechanism of PI, while photochemical activities are more important for the TP. The combination of phase masks and the TP allows an efficient fabrication of three-dimensional topographies using laser ablation. The TP also reveals superior properties for applications in the near-IR. The carbon-doped polymer shows properties that are useful for the application of polymers in laser plasma thrusters for microsatellites.

Keywords: Photopolymer; Ablation; Microoptic; Phase mask; Laser plasma thruster

1. Introduction

Laser ablation of polymers was first reported in 1982 [1,2] and envisioned as a possible alternative or complementary technique to conventional photolithography, but has unfortunately several disadvantages, i.e., low sensitivity [3], carbonization upon irradiation [4], and debris contaminating the surface [5] and optics. These problems are mainly the result of the application of standard polymers. Therefore, novel photopolymers were developed for ablation at a specific irradiation wavelength, i.e., 308 nm, to overcome these limitations [6–10]. Photochemical considerations, i.e., photolabile groups in the polymer main chain, have been applied for the design of these polymers. The irradiation wavelength of 308 nm was chosen because of the convenience of this wavelength from a practical

* Corresponding author. Tel.: +41-56-3104076; fax: +41-56-3102485.
E-mail address: thomas.lippert@psi.ch (T. Lippert).

0169-4332/02/$ – see front matter
PII: S0169-4332(01)00656-0

point of view, i.e., lifetime of the optical components and gas fills of the XeCl excimer laser, and because sub-micron resolution is not necessary for all applications. The irradiation wavelength of 308 nm is mainly absorbed by the photochemically active chromophore. It is therefore possible to selectively decompose the polymer at pre-determined positions. This can give indications about the role of the photochemically active chromophore during the ablation process and, therefore, the ablation mechanism. It is still not clear whether the ablation mechanism is purely photothermal or has at least partly photochemical features. The latter has been suggested for shorter irradiation wavelengths, e.g., 193 nm [11]. The photopolymers are highly absorbing at the irradiation wavelength and decompose exothermally at well-defined positions of the polymer chain into gaseous products [12]. The gaseous products act as driving gas of ablation and carry away larger fragments, which could otherwise contaminate the surface. The polymers are ablated without major modifications of the residual polymer surface [13], thus allowing reproducible ablation.

For this study, three designed polymers (structures shown in Scheme 1) and one commercial polymer, i.e., polyimide (PI), as reference were selected. The designed polymers are:

- Triazene-polymer (TP), with two triazene (–N=N–N< >) groups per repetition unit.
- Polyester with a cinnamylidenmalonic ester (CSMP) group, that can be crosslinked to act as negative type photoresist [14].
- Polyester (TCP), which contains two triazene groups per repetition unit plus the cinnamylidenmalonic ester group.

All of these polymers, including PI, have similar absorption coefficients ($\approx 97\,000 \pm 5000\,\mathrm{cm}^{-1}$) at the irradiation wavelength (308 nm). The polymer that revealed the highest etch rate (lowest threshold) was selected for additional studies at low fluences. Low fluences are the most interesting range of ablation, because additional processes during ablation, such as plasmas and inverse Bremsstrahlung, are only pronounced at higher fluences.

Laser ablation has the potential to become an important tool for the fabrication of complex patterns, e.g., microoptical elements. These can either be generated by scanning ablation tools, which are even capable of producing continuous topographies by varying the applied fluence on the material surface [15]. Due to the sequential nature of the method, the throughput is very limited. A parallel patterning of larger areas requires a set-up comparable to photo steppers, where the mask structure is projected onto the substrate surface [16]. Diffractive grating structures (phase masks) etched into a quartz mask blank can be used to diffract the transmitted light out of the aperture of the projection optics [17], allowing the fabrication of complex patterns. The phase masks exhibit long lifetimes compared to the conventional Cr-absorber mask, which can be damaged by the laser. The combination of laser ablation with phase masks merges the capability of scanning ablation tools to vary the ablated depth continuously with the high throughput of projection methods. An additional improvement can be achieved by the application of special photopolymers.

A very different application of laser ablation of polymers can be found in aerospace science. With the advent of microsatellites (>10 kg), nanosatellites (1–10 kg) and even picosatellites (<1 kg), it is necessary to develop steering engines, which have a small mass ($\leq$200 g) and size, produce a high specific

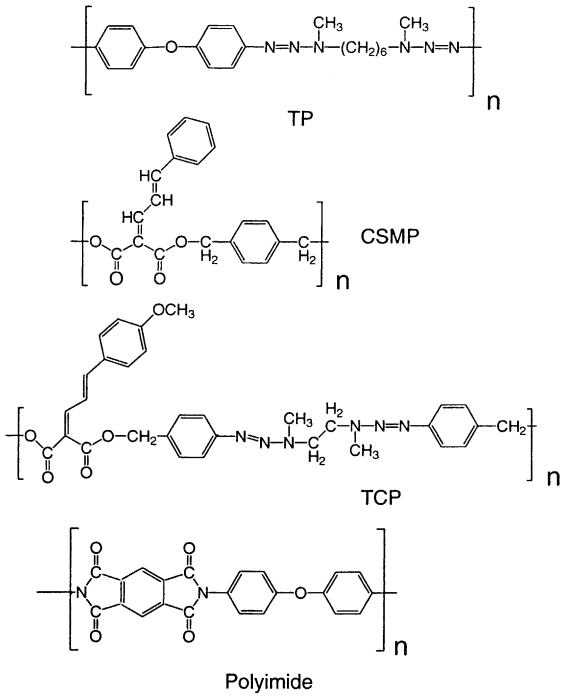

Scheme 1. Chemical structures of the polymers.

impulse and are inexpensive. One promising candidate for this application are laser plasma thrusters (LPTs) [18,19], which have some advantages over more common candidates for microthrusters, such as pulsed plasma thrusters or resistojets. Due to the specific demands, i.e., weight and power, of small satellites, small powerful ($\geq$1 W) diode lasers must be used. These lasers emit in the near-IR (930–980 nm) with an available power of around 1–5 W and pulse lengths from 100 μs to the millisecond range. Fluences of several hundred joules per square centimeters can be achieved with standard optical components (laser spot diameter around 5 μm). The long pulse lengths of the diode lasers restrict the applicable materials to polymers, which have low thermal conductivities. The performance of the LPTs, to a large extent, depends on the properties of the polymers used in these devices. The well-defined exothermic decomposition of the above-mentioned photopolymers was an attractive feature to test these polymers also for an application with near-IR irradiation.

2. Experimental

The polymers, TP, CSMP and TCP (Scheme 1) were synthesized using standard polycondensation reactions. The syntheses are described in detail elsewhere [20,21]. Thin sheets (125 μm, Kapton® from Goodfellow) or spincoated PI films (Durimide 7020, Arch Chemical) were used. A XeCl excimer laser (Lambda Physik, Compex 205; $\lambda = 308$ nm, $\tau = 20$ ns) was used as irradiation source for most experiments, with the exception of the interference experiments (see below). The polymer films (50 μm thick) for the laser ablation experiments were prepared by solvent casting with THF or chlorobenzene as solvent. The procedure for determining the etch rates has been described in detail elsewhere [22]. The ablation experiments were performed at low (10–400 mJ cm^{-2}) and high fluences (up to 20 J cm^{-2}) to investigate the ablation behavior.

The experimental arrangement for the UV–Vis [23] and the time-of-flight mass spectrometer (TOF-MS) measurements [24] has been described previously.

The experimental set-up for the time-resolved (ns) surface interference fringes has been described in detail elsewhere [25]. Briefly, the second harmonic of a Q-switched Nd:YAG laser (Continuum Surelite I, 532 nm, 10 ns FWHM) was used as probe light source of the interferometer to measure the excimer laser-induced morphological changes of the polymer films. The interference patterns were captured by a CCD camera (Sony, XC77, 512 × 512 pixels) and then analyzed. Time-resolved measurements were carried out by controlling the delay time (Δt) between the excitation and probe laser pulses with a digital delay/pulse generator (Stanford Research System, DG 535). Here we define $\Delta t = 0$ when the peaks of both laser pulses overlap completely. Different to all other experiments, a XeF excimer laser (Lambda Physik Lextra 200, 351 nm, 30 ns FWHM) was used as excitation source.

Thin films (1–5 μm thick) of the TP were spincoated onto quartz wafers for the fabrication of micro-optical elements. As spincoating solution 15 wt.% of the polymer in chlorobenzene were used. The PI (125 μm thick sheets of Kapton® from Goodfellow) was used as received. The phase masks were prepared by electron beam lithography, as reported elsewhere [26].

For the carbon-doped TP films, chlorobenzene was used as solvent, while for the carbon-doped polyvinylalcohol (PVAlc, Alcotex™, Hoechst) a water/methanol mixture was used. The polymer solutions were combined with carbon (0.5 wt.%, Ketjen Black, BASF) suspensions (prepared with a high speed stirrer, Ultra-Turrax T25, in the same solvent as the polymer) and mixed with the high-speed stirrer. The films ($\geq$60 μm) were prepared by drawing (draw blade applicator, Industry Tech) the suspensions onto polymer substrates (PET). The performance of the films was determined by irradiation with a diode laser (SDL XC30) and a special developed torsion balance (sensitivity as low as 10^{-10} N s), described in detail elsewhere [19].

3. Results and discussion

3.1. Ablation characteristics

The high fluence range is mainly interesting for applications where high ablation rates in small areas are important, e.g., drilling or cutting. The low fluence range offers the opportunity to study the influence of

structural parameters on the ablation rates. The low fluence range is also important for lithographic applications, where the cost of the photons is important. Low fluences are defined in this study from 10 to 500 mJ cm^{-2}. The etch rates (etch depth/pulse) were calculated from linear plots of the etch depths versus pulse number at a given fluence. All plots were linear, showing no incubation behavior as expected for highly absorbing polymers. A plot of the etch rates versus high (top) and low (bottom) fluences (not the normally applied logarithmic fluence scaling) is shown in Fig. 1. Clear differences between the etch rates of all polymers are observed in the low fluence range. The designed polymers (CSMP, TCP and TP) can be divided into two groups with respect to the etch rates. All triazene-containing polymers have significantly higher etch rates than the other polymers. The designed polyester (CSMP) reveals also a higher etch rate than PI. The etch rate is independent from α_{lin} (similar for all polymers) and determined by the chemical structure. The highest etch rate is obtained for TP, which has the highest triazene density per polymer chain. The same trend is also observed at high fluences (Fig. 1, top). This feature is not very pronounced in plots using the standard logarithmic fluence scale. The TP polymer shows a remarkably high etch rate of more than 3 μm per pulse at the highest applied fluences.

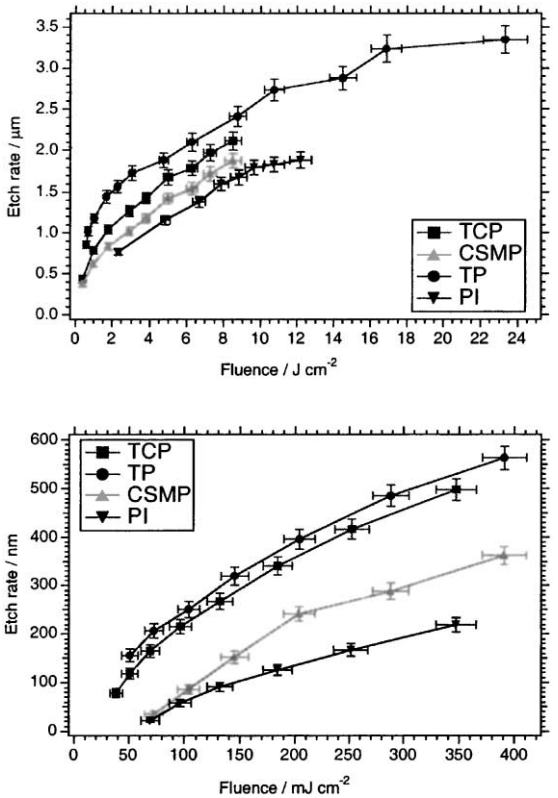

Fig. 1. Measured etch rates as a function of the fluence at high fluences (top) and low fluences (bottom).

The effective absorption coefficient α_{eff} and threshold fluence F_{th} were calculated at low fluences according to the following equation [27,28]:

$$d(F) = \frac{1}{\alpha_{eff}} \ln\left(\frac{F}{F_{th}}\right) \quad (1)$$

where $d(F)$ is the etch rate (etch depth per pulse). For all designed polymers similar α_{eff} of $\approx 54\,000 \pm 5000\,\text{cm}^{-1}$ are obtained, while PI has an α_{eff} of about 83 000 cm^{-1}. The effective absorption coefficients of the designed polymers are quite different from the linear absorption coefficients, whereas the values for PI are comparable. The threshold fluences range from $27 \pm 2\,\text{mJ cm}^{-2}$ (for TP and TCP) to $60 \pm 5\,\text{mJ cm}^{-2}$ for CSMP and PI. Well-defined, clean ablation structures are obtained for the designed polymers, while in the case of PI carbon-debris is detected in and around the ablation structures [4]. An example of a structure created into TP with 50 (top) and 10 pulses at a fluence of 200 mJ cm^{-2} is shown in Fig. 2. The structure is created by imaging a slit mask onto the sample surface, using a Schwarzschild type reflecting objective with a demagnification of 25:1. The ablation structures are very well-defined with no visible heat affected zone or debris contaminating the surrounding of the structures.

3.2. Low fluence irradiation

The polymer with the highest etch rates and lowest F_{th}, i.e., TP, was selected to study the ablation mechanism in more detail with various experimental techniques. The low fluence range was chosen to determine whether photochemical features are important during laser ablation. In Fig. 3, the UV–Vis absorption spectra of a thin TP film is shown. Thin (<1 μm) TP films were irradiated with various fluences and the absorption at 330 nm, corresponding to the triazene chromophore [23], was measured before

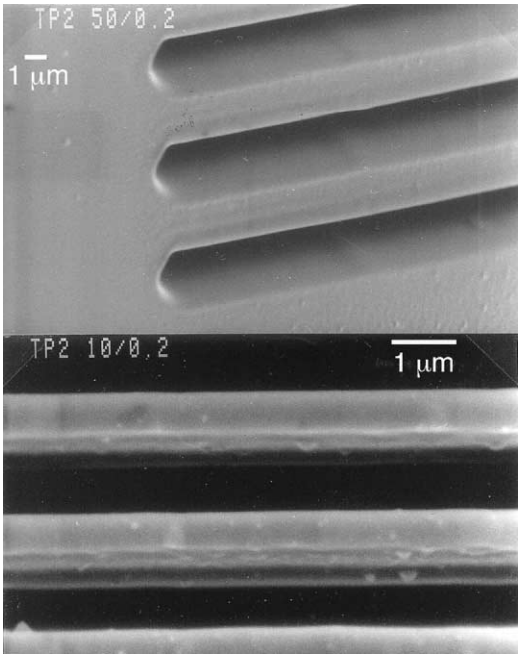

Fig. 2. SEM micrographs of microstructures in the TP: 50 pulses with 200 mJ cm^{-2} (top) and 10 pulses with 200 mJ cm^{-2} (bottom) (from Ref. [7]).

and after each irradiation with a UV–Vis spectrometer. The changes of the absorption, ΔA, normalized by the applied fluence are plotted versus the fluence (Fig. 4). Three features are clearly visible:

- Decomposition of the triazene-chromophore with fluences below the threshold of ablation ($\Delta A \neq 0$).
- Sharp increase of ΔA between 20 and 25 mJ cm^{-2}, agreeing very well with the threshold determined by Eq. (1).
- Nearly constant ΔA for fluences slightly above the threshold of ablation.

The values of ΔA below the threshold of ablation confirm that the photolabile triazene group decomposes as expected for a photolabile group. The linear range of the fluence-normalized ΔA indicates also a linear photochemical reaction. The quantum yield (QY) is around 2%, which is about a factor of 10 higher than in solution. The conformity of the threshold fluences determined by the different methods is at least indicating that the film thickness (at least in the range <1 μm for the UV–Vis experiments versus the ≥200 μm for the ablation studies) is not important. The more or less linear fluence normalized ΔA values just above the threshold of ablation suggest that ablation may start as a linear process even if this is not clearly visible in etch rate plots (Fig. 1). The changes in ΔA correspond to a QY of about 30%, which is again a factor of 10 higher than for films irradiated with fluences below the threshold of ablation.

A similar fluence range was also studied by TOF-MS. In these experiments, the main product, i.e., N_2,

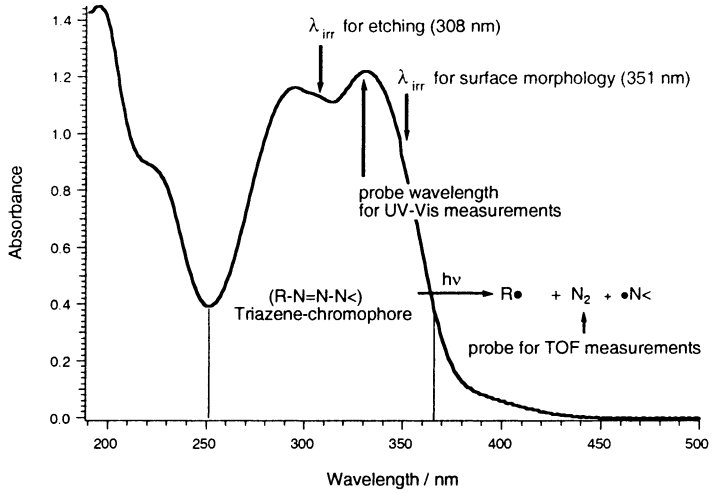

Fig. 3. UV–Vis absorption spectra of the TPs. Thin film coated from chlorobenzene onto a quartz wafer. The irradiation wavelengths and probes for the different experiments are shown as insets.

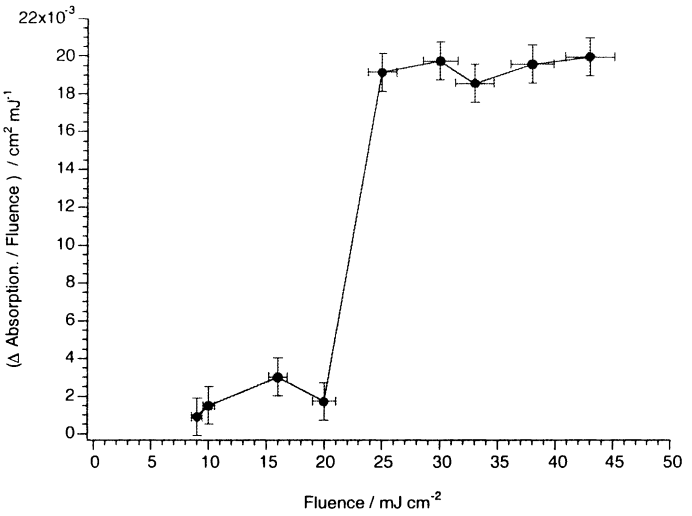

Fig. 4. Change of absorbance, ΔA of thin polymer films (<1 μm) before and after laser irradiation (308 nm). The values are normalized with the applied fluence and plotted versus the fluence (from Ref. [23]).

of the decomposition of the triazene group is used as probe for the decomposition of the triazene group. The primary decomposition step [29] is presented as inset in Fig. 3. Fig. 5 shows the peak intensity of the nitrogen versus the applied laser fluence. Similar features as in the UV–Vis measurements are visible. The decomposition product, N_2, is detected for irradiation with fluences below the threshold of ablation. The peak intensity of the nitrogen increases linearly up to ≈35 mJ cm^{-2}, then a steep, linear increase of the peak intensity is detected. It is remarkably that the value of ≈35 mJ cm^{-2}, obtained with a very different

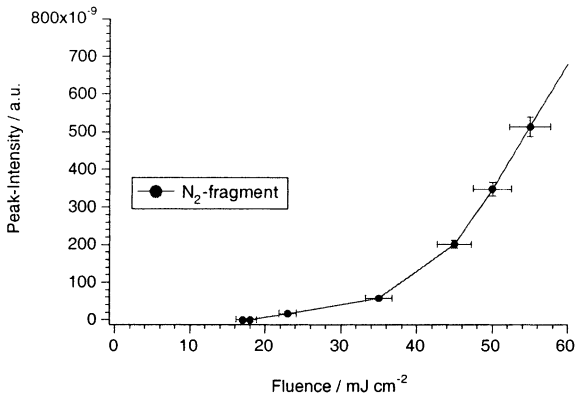

Fig. 5. Intensity of the 28 amu (N_2) signal from decomposition of the TP at various fluences with 308 nm irradiation.

method, corresponds again very well with the previously determined values for the threshold fluence. This also suggests that the atmosphere has only minor influence on the ablation of the TP, because the former experiments are performed in air, while the TOF-MS measurements are performed in ultra-high vacuum.

The UV–Vis and TOF-MS experiments strongly indicate that photochemical reactions are important in the low fluence range (below and just above the threshold of ablation). Another technique that can give indications about the ablation mechanism is nanosecond interferometry. It has been shown in previous studies [30,31] that thermal/photothermal ablation results first in pronounced swelling of the polymer surface, followed by etching. The etching takes place on time scales much longer than the pulse length of the excimer laser (up to the microsecond range). TP and PI were studied with an irradiation wavelength of 351 nm. The ablation threshold for TP at 351 nm is also 25 mJ cm^{-2}, while PI exhibits a threshold of 210 mJ cm^{-2}. The experiments were performed with fluences above the threshold of ablation, i.e., 225 mJ cm^{-2} for TP and 460 mJ cm^{-2} for PI. The results are shown in Fig. 6. The etching of the TP starts and ends within the excitation pulse of the excimer laser. Prior to etching, darkening of the surface is observed, which is probably due to the creation of the first products, i.e., N_2, inside the polymer [32]. The

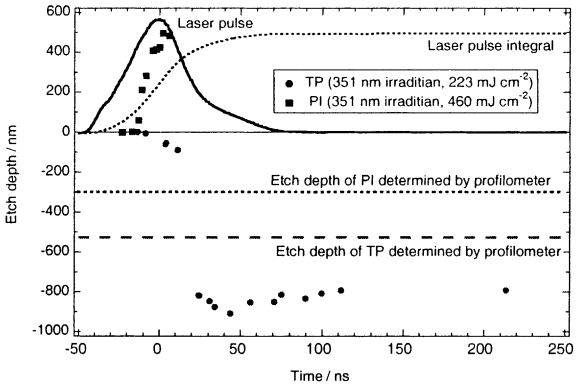

Fig. 6. Nanosecond expansion/etching behavior of the TP and PI after 351 nm irradiation.

overestimation of the etch depths is due to the experimental configuration, described in detail elsewhere [32]. In the case of PI, a very different behavior is observed. It was only possible to observe swelling of the polymer surface (up to several hundred nanometers), but time resolved etching or swelling after several nanoseconds could not be observed, probably due to the ejection of fragments which shield the probe light.

The differences between TP and PI in the dynamic interferometric studies suggest again that different mechanisms are active for TP and PI. We have strong indication for a partly photochemical ablation mechanism for TP, i.e., products of decomposition at low fluences, sharp threshold and clean etching within the time scale of the laser pulse. In the case of PI, a photothermal mechanism is more probable, e.g., swelling and etching on time scales longer than the laser pulse.

3.3. Novel applications

3.3.1. Microoptical elements: UV-irradiation

The phase masks were designed for 308 nm as irradiation wavelength using an 80 mm focal length projection lens at demagnification factors between 2 and 4. Only the 0th order was used for the structuring (higher orders were blocked by an aperture). The 0th order efficiency of the phase masks was calculated by scalar diffraction theory with incorporation of the nonlinear ablation behavior and threshold fluence into the mask design. This improves the efficiency of the ablated structures, e.g., diffraction efficiency of gratings, by a factor of 2 [17].

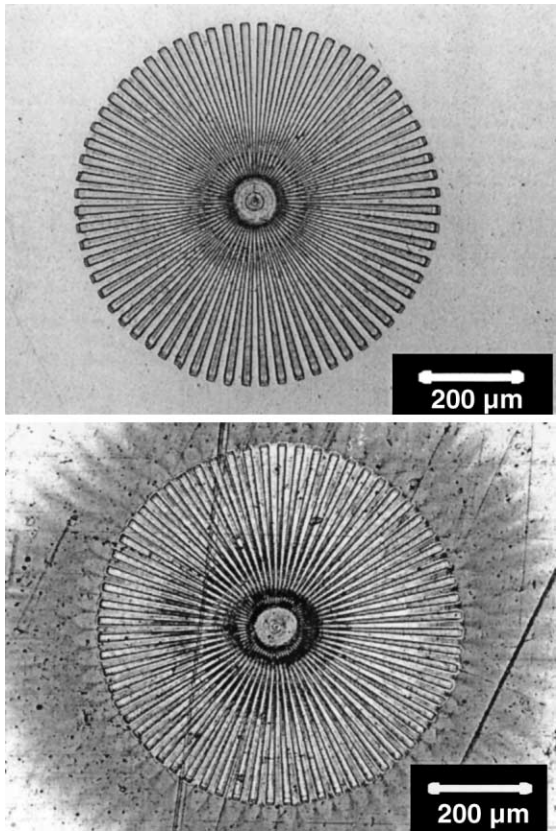

Fig. 7. SEM images of Siemens stars fabricated by laser ablation. Siemens stars in the TP (top) and PI (bottom) using 5 pulses at 308 nm.

Various structures were ablated into TP and PI. An example of a Siemens star etched into the TP (top) and PI (bottom) is shown in Fig. 7. The modified and redeposited material is clearly visible around the ablated structure of the PI (bottom), but is absent for the TP (top). Any surface contamination or modification will deteriorate the performance of the microoptical elements and render the ablation rates unpredictable. The higher sensitivity and etch rates of the TP allows the application of larger phase masks. Alternatively, less pulses are necessary to fabricate an optical element with a given depth of the structures.

The combination of gray tone phase masks with the highly sensitive photopolymers is suitable for the fast fabrication of three-dimensional topographies. Single

laser pulses can create complex structures, such as Fresnel lenses or lens arrays [17]. A pattern transfer into glass or quartz, e.g., by proportional etching techniques, would open an even larger spectrum of applications.

3.3.2. Laser plasma thruster: near-IR irradiation

One property of the designed polymers is the exothermic decomposition and the 'weak' =N–N< bond in the polymer. This weak bond is probably also the primary decomposition site for near-IR irradiation wavelengths, which will result in thermal decomposition. To analyze the performance of the polymer films for LPTs (cf. Section 1), the target momentum was measured by the torsion balance and used to calculate the momentum coupling coefficient, C_m. This quantity is defined as

$$C_m = \frac{m\Delta v}{W} \quad (2)$$

with $m\Delta v$ as the target momentum produced during the ejection of laser-ablated material. W is the incident laser pulse energy. Another important parameter for thrusters is the specific impulse I_{sp}, which is defined as

$$C_m Q^* = v_E = I_{sp} g \quad (3)$$

where Q^* is the specific ablation energy (incident power/mass ablation rate), v_E the exhaust velocity and g the acceleration due to gravity. In other words, I_{sp} is the time for which an acceleration of g would have to act to bring the exhaust mass up to the velocity v_E. For chemical rockets, the maximum impulse is about 500 s, limited by the available temperatures, while a specific impulse of 8000 s was reported for laser ablation of Al [33]. Two polymers were selected for the tests, i.e., a polymer designed for laser ablation (TP) in the UV and a commercial polymer (PVAlc). Both polymers pass the fundamental requirements for LPTs. The polymers give homogenous films with a good adhesion on PET; they do not stick to each other; they are elastic over a broad temperature range (−50 to +60 °C) and have an optical density (OD) of about 1. The latter requires that it is possible to dope the films homogenously with carbon. Carbon was chosen as dopant due to the broad homogenous absorption over the whole near-IR range. The films of both the polymers were prepared with an OD of ≈0.9 and a thickness of around 60 μm. The film thickness is the upper limit that can be accomplished for these polymers by our preparation method and tools.

In Fig. 8, the momentum coupling coefficients and specific impulse at various laser fluences of the carbon-doped triazene polymer and of a carbon-doped PVAlc are shown. The TP reveals higher coupling coefficients and, more importantly, a quite well defined threshold for a maximum C_m. The carbon-doped triazene polymer clearly reveals a higher specific impulse than the PVAlc. The fewer data points for

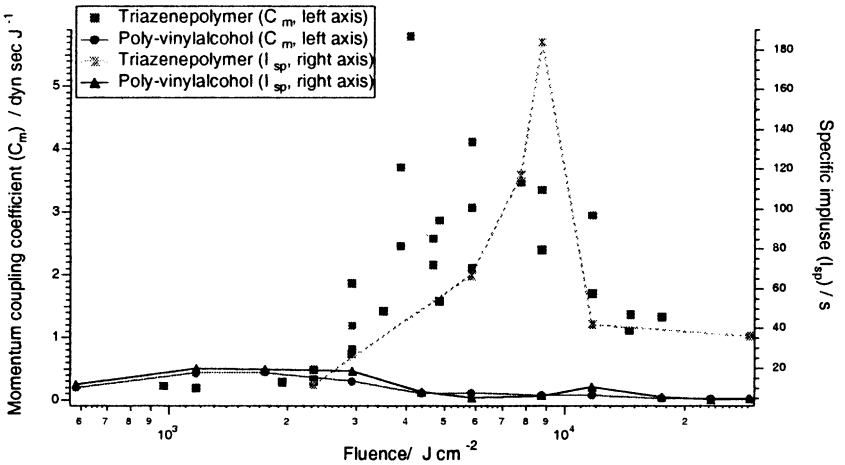

Fig. 8. Momentum coupling coefficient (impulse/laser energy) and specific impulse at various fluences for the carbon-doped polymers (TP and PVAlc). OD at 935 nm ≈0.9, film thickness ≈65 μm, PET substrates.

the triazene polymer are due to the very irregular shape of the craters which did not allow measurements of the ablated volume at all laser fluences. The I_{sp} values are clearly higher for the TP, and probably reveal a maximum at a similar fluence range as for C_m.

4. Conclusions

The ablation characteristics of various polymers were studied at low and high fluences. The polymers can be divided into three groups, polymers containing triazene groups, polyesters with cinnamylidenemalonyl groups, and PI as reference polymer. The polymers containing the photochemically most active group (triazene) are also the polymers with the lowest threshold of ablation and the highest etch rates, followed by the designed polyesters and then PI. No pronounced influences of the absorption coefficients, neither α_{lin} nor α_{eff}, on the ablation characteristics are detected. The TP was studied with additional techniques at low fluences. UV–Vis spectroscopy reveals that the triazene-chromophore decomposes also upon irradiation with fluences clearly below the threshold of ablation. At the threshold fluence, a pronounced change is detected, i.e., an approximately 10 times higher decomposition rate. The TOF-MS measurements reveal also a decomposition of the triazene-unit at fluences below the threshold of ablation. This was monitored by detecting the main decomposition product of the triazene group, i.e., N_2. The amount of detected nitrogen increases drastically above the threshold of ablation which is consistent with the UV–Vis measurements. The comparison of the surface morphology of the TP and PI after irradiation with fluences above the threshold of ablation reveals pronounced differences. In the case of the TP, no swelling of the surface is observed and the etching starts and ends with the laser pulse, while a very pronounced swelling is detected for PI. The clear difference between PI and the designed polymers is probably due to the pronounced thermal part in the ablation mechanism of PI, while photochemical activities are more important for the TP.

The combination of phase masks and specially designed, highly sensitive photopolymers can be used for an efficient fabrication of three-dimensional topographies using laser ablation. The application of the TP, which has a very low threshold fluence, a high ablation rate and a decomposition without surface contamination, allows a fast fabrication of microoptical elements. The TP reveals also superior properties for applications in the near-IR. The carbon-doped polymer shows higher values of the momentum coupling coefficient (impulse of ablated products divided by laser energy) compared to a commercial polymer (PVAlc). The well-defined threshold for the momentum coupling coefficient is an important feature for the application of polymers in LPTs for microsatellites.

Acknowledgements

This work has been supported by the Swiss National Science Foundation, a NATO Grant for international collaboration (CRG 973063), and by the US Air Force Office of Scientific Research (STTR Phase II contract No. F49620-98-C-0038).

References

[1] R. Srinivasan, V. Mayne-Banton, Appl. Phys. Lett. 41 (1982) 576.
[2] Y. Kawamura, K. Toyoda, S. Namba, Appl. Phys. Lett. 40 (1982) 374.
[3] K. Suzuki, M. Matsuda, T. Ogino, N. Hayashi, T. Terabayashi, K. Amemiya, Proc. SPIE 2992 (1997) 98.
[4] F. Raimondi, S. Abolhassani, R. Brütsch, F. Geiger, T. Lippert, J. Wambach, J. Wei, A. Wokaun, J. Appl. Phys. 88 (2000) 1.
[5] R. Srinivasan, B. Braren, R. Dreyfus, J. Appl. Phys. 56 (1987) 372.
[6] T. Lippert, J. Stebani, J. Ihlemann, O. Nuyken, A. Wokaun, Angew. Makromol. Chem. 206 (1993) 97.
[7] T. Lippert, J. Stebani, J. Ihlemann, O. Nuyken, A. Wokaun, J. Phys. Chem. 97 (1993) 12296.
[8] T. Lippert, T. Kunz, C. Hahn, A. Wokaun, Recent Res. Dev. Macromol. Res. 2 (1997) 121.
[9] O. Nuyken, U. Dahn, N. Hoogen, D. Marquis, M.N. Nobis, C. Scherer, J. Stebani, A. Wokaun, C. Hahn, Th. Kunz, T. Lippert, Polym. News 24 (1999) 257.
[10] O. Nuyken, C. Scherer, A. Baindl, A.R. Brenner, U. Dahn, R. Gärtner, S. Kaiser-Röhrich, R. Kollefrath, P. Matusche, B. Voit, Prog. Polym. Sci. 22 (1997) 93.
[11] S. Küper, J. Brannon, K. Brannon, Appl. Phys. A 56 (1993) 43.
[12] L.S. Bennett, T. Lippert, H. Furutani, H. Fukumura, H. Masuhara, Appl. Phys. A 63 (1996) 327.
[13] T. Lippert, T. Nakamura, H. Niino, A. Yabe, Macromolecules 29 (1996) 6301.

[14] T. Lippert, J. Wei, A. Wokaun, N. Hoogen, O. Nuyken, Macromol. Mater. Eng. 283 (2000) 140.
[15] N.H. Rizvi, P.T. Rumsby, M.C. Gower, Proc. SPIE 3898 (1999) 240.
[16] E.C. Harvey, P.T. Rumsby, Proc. SPIE 46 (1998) 26.
[17] C. David, J. Wei, T. Lippert, A. Wokaun, Microlectr. Eng. 57–58 (2001) 453.
[18] C.R. Phipps, J. Luke, Proc. SPIE 4065 (2000) 801.
[19] C. Phipps, J. Luke, Diode laser-driven microthrusters: A new departure for micropropulsion, AIAA J., Vol. 401, no. 1, January 2002.
[20] O. Nuyken, J. Stebani, T. Lippert, A. Wokaun, A. Stasko, Macromol. Chem. Phys. 196 (1995) 739.
[21] N. Hoogen, O. Nuyken, J. Polym. Sci. Polym. Chem. 38 (2000) 1903.
[22] J. Wei, N. Hoogen, T. Lippert, O. Nuyken, A. Wokaun, J. Phys. Chem. B 105 (2001) 1267.
[23] T. Lippert, L.S. Bennett, T. Nakamura, H. Niino, A. Ouchi, A. Yabe, Appl. Phys. A 63 (1996) 257.
[24] J.J. Shin, D.R. Ermer, S.C. Langford, J.T. Dickinson, Appl. Phys. A 64 (1997) 7.
[25] H. Furutani, H. Fukumura, H. Masuhara, Appl. Phys. Lett. 65 (1994) 3413.
[26] C. David, D. Hambach, Microelectr. Eng. 46 (1998) 219.
[27] J.E. Andrews, P.E. Dyer, D. Forster, P.H. Key, Appl. Phys. Lett. 43 (1983) 717.
[28] R. Srinivasan, B. Braren, J. Polym. Sci. 22 (1984) 2601.
[29] T. Lippert, S.C. Langford, A. Wokaun, S. Georgiou, J.T. Dickinson, J. Appl. Phys. 86 (1999) 7116.
[30] H. Furutani, H. Fukumura, H. Masuhara, J. Phys. Chem. 100 (1996) 6871.
[31] H. Furutani, H. Fukumura, H. Masuhara, S. Kambara, T. Kitaguchi, H. Tsukada, T. Ozawa, J. Phys. Chem. B 102 (1998) 3395.
[32] H. Furutani, H. Fukumura, H. Masuhara, T. Lippert, A. Yabe, Phys. Chem. A 101 (1997) 5742.
[33] C.R. Phipps, M.M. Michaelis, Laser Part. Beams 12 (1994) 23.